

# Comparison of laser-assisted charge transfer of symmetric and asymmetric colliding systems

**F. J. Domínguez-Gutiérrez and R. Cabrera-Trujillo**

Instituto de Ciencias Físicas, Universidad Nacional Autónoma de México, Ap. Postal 43-8,  
Cuernavaca, Morelos, 62251, México

E-mail: javier@fis.unam.mx, trujillo@fis.unam.mx

**Abstract.** We study the effect of an intense, ultra-short, and ultra-fast (1 and 2 fs) pulse with the aim to manipulate the charge transfer process of symmetric and asymmetric colliding systems. We report the total and state-selective cross section for charge transfer for the symmetric  $H^+ + H$  and for the asymmetric  $He^{2+} + H$  system by means of the Crank-Nicolson method in the energy collision range for 1-10 keV/amu and 0.25-10 keV/amu, respectively. In this work, we show that the laser assistance do minimal contribution to charge transfer process in the symmetric system and that the laser pulse increases the charge transfer process at low impact energies for asymmetric system up to an order of magnitude. To assess the validity of our results, we compare our numerical results for the case of collisions with no laser to available experimental data in the literature showing good agreement for both systems.

## 1. Introduction

The charge transfer process in collisions between bare ions as projectiles and one electron atomic targets is an important process in determining the radiation losses and neutral beam heating efficiencies of plasmas in Tokamak [1]. Nowadays, laser assisted have been suggested to improve the charge transfer process in ion-atom collisions [2, 3, 4, 5, 6] with the aim to manipulate and control the electron capture process. The laser assisted collision for resonant symmetric systems have been studied by Ferrante et al. [7] by using the impact parameter method and the atomic two-state approximation for the resonant systems  $H^+ + H$  and  $Rb^+ + Rb$  finding that the effect of the laser on the total charge transfer process is to enhance it in a small order. Meanwhile a numerically treatment of the symmetric system  $H^+ + H$  with a laser assistance is done by Niederhausen et al. [5] solving the time dependent Schrödinger equation finding a strong laser-phase dependence for charge transfer processes, and weak evidence for a charge-resonant enhanced ionization process for a circular polarized laser pulse. A study of the asymmetric system  $He^{2+} + H$  considering a laser assisted collision is done by Kirchner [9] finding that the laser enhances the total charge transfer process at low impact energy collision with a dependence on the initial phase of the laser.

The purpose of this work is to compare the effect of an ultra-fast, ultra-short and intense laser pulse on the state selective charge transfer process considering a symmetric  $H^+ + H$  and asymmetric  $He^{2+} + H$  collisions systems at intermediate impact energy collisions.

Our work is organized as follows. In Sec. 2, we define the Hamiltonian that describes the dynamics of the laser-assisted ion-atom collision. In Sec. 2.1 we describe our method to obtain the electronic states for the projectile and target. In Sec. 2.2, the dynamics of the electron during



the collision is obtained by solving the time-dependent Schrödinger equation by means the finite difference method. In Sec. 2.3, we describe the numerical implementation of our finite-difference procedure. In Sec. 2.4, we show the procedure to obtain the charge transfer cross section within the finite-differences approach. At the end of this section, we describe the implementation of the initial conditions of the dynamics of the collision with laser assisted collision to obtain the charge transfer probability. In Sec. 3, we report our numerical results for the state selective charge transfer cross-section of the symmetric and asymmetric collision systems with and without laser assistance. There we show a good agreement between our laser-free numerical data and the results reported in the literature by other theoretical methods and experimental data for both collision systems. Finally a brief summary is given in Sec. 4. Atomic units are used throughout unless otherwise noted.

## 2. Theory

We consider a system with a bare projectile ion ( $Z_p$ ) moving on a straight-line trajectory colliding with an atomic hydrogen target. The Hamiltonian that describes the dynamics of the electron is

$$\mathbf{H} = -\frac{1}{2}\nabla^2 - \frac{1}{|\mathbf{r}|} - \frac{Z_p}{|\mathbf{r} - \mathbf{R}(t)|} - \mathbf{r} \cdot \mathcal{E}(t), \quad (1)$$

where the first term in Eq. (1) corresponds to the kinetic energy operator  $\mathbf{T} = -\frac{1}{2}\nabla^2$ , the second term is the interaction potential between the electron and the target, and the third term is the interaction potential between the electron and the projectile. The straight-line trajectory projectile is defined by  $\mathbf{R}(t) = (b, 0, v_p t)$ , where  $b$  is the impact parameter and  $v_p = \sqrt{2E_p/m_p}$  is the projectile velocity. Finally, the fourth term is the semi-classical description of the electron-laser electric field coupling in the dipole-length representation. We model the laser pulse by a Gaussian envelope as

$$\mathcal{E}(t) = \mathcal{E}_0 \exp\left(-\frac{t^2}{\tau^2}\right) \cos(\omega t + \phi), \quad (2)$$

where  $\mathcal{E}_0$  defines the polarization vector of the laser pulse which in our case is placed in the plane of the collision along the projectile velocity. The intensity at full width half-maximum (FWHM) is given by  $\tau\sqrt{4\ln 2}$ , such that  $\tau$  defines the duration of the pulse,  $\omega$  is the carrier frequency and  $\phi$  is the relative collision laser phase (RCLP). The RCLP combines both the carrier-envelope phase of the laser as well as the synchronization of the laser pulse with the collision.

### 2.1. Stationary states of the projectile bare ion

We use the finite-differences method to solve the time-independent Schrödinger equation (TISE) to obtain the neutral hydrogen atom and  $\text{He}^+$  ion stationary states at the end of the collisions, with the following Hamiltonian

$$\mathbb{H} = -\frac{1}{2}\nabla^2 - \frac{Z}{|\mathbf{r}|}, \quad (3)$$

where  $Z = 1$  or  $2$  for the H or  $\text{He}^+$  atom, respectively. To solve the previous equation, we propose a solution in spherical coordinates as  $\Phi(\mathbf{r}) = D(r)Y_{l,m}(\theta, \phi)$ . For the radial part,  $D(r)$ , we use the change of variable  $D(r) = \zeta(r)/r$  obtaining the following differential equation

$$\left(-\frac{1}{2}\frac{d^2}{dr^2} - \frac{l(l+1)}{2r^2} - \frac{Z}{r}\right)\zeta(r) = E\zeta(r). \quad (4)$$

Now, we discretize the function  $\zeta(r)$  and the second derivative of the function  $\zeta(r)$  of Eq. (4) in a numerical grid as  $\zeta(r) \rightarrow \zeta_k$  when  $r \rightarrow r_k$  on the  $k$ -points in the numerical grid, with an

uniform spacing  $\Delta r$ . By considering the  $\zeta_k$  points as the elements of a N-dimensional vector, we rewrite the previous equations as an eigenvalue problem, that is

$$\mathbb{B}\vec{\zeta} = E\vec{\zeta} \quad (5)$$

where the matrix  $\mathbb{B}$  has the following elements

$$\begin{pmatrix} 2B + V_{\text{eff}_1} & -B & 0 & \dots & 0 \\ -B & 2B + V_{\text{eff}_2} & -B & \dots & 0 \\ \vdots & \vdots & \vdots & \ddots & \vdots \\ 0 & \dots & 0 & -B & 2B + V_{\text{eff}_N} \end{pmatrix}. \quad (6)$$

Here  $V_{\text{eff}_i}$  is the discretization of the effective potential  $V_{\text{eff}} = -l(l+1)/2r^2 - Z/r$  and  $B = 1/2\Delta r^2$ . From Eq. (5) we can obtain the values for the bound-energies and the numerical eigen-functions of the neutral H atom or  $\text{He}^+$  ion.

## 2.2. Dynamics of the electron during the collision

The total wave function  $\Psi(\mathbf{r}, t)$  describes the dynamics of the electron cloud in the collision and it is obtained by solving the time-dependent Schrödinger equation (TDSE)

$$\mathbf{H}\Psi(\mathbf{r}, t) = i\frac{\partial}{\partial t}\Psi(\mathbf{r}, t), \quad (7)$$

with the Hamiltonian in Eq. (1). The solution to Eq. (7) is given by the unitary propagator operator as

$$\Psi(\mathbf{r}, t) = \exp(-i\mathbf{H}\Delta t)\Psi(\mathbf{r}, t_0). \quad (8)$$

where  $t_0$  and  $t$  are the initial and final time, respectively, and  $\Delta t = t - t_0$ . The propagation in time is obtained by implementing the Crank-Nicolson and the finite-differences methods. Then, we consider the Hamiltonian as  $\mathbf{H} = \mathbf{T} + \mathbf{V}$  with the kinetic energy operator as  $\mathbf{T} = \sum_{\eta} \mathbf{T}_{\eta}$

where  $\eta = x, y, z$ , such that the unitary propagator operator becomes

$$\prod_{\eta} \exp\left(\frac{i}{2}\mathbf{T}_{\eta}\Delta t\right)\Psi = \prod_{\eta} \exp\left(-\frac{i}{2}\mathbf{T}_{\eta}\Delta t\right)\Xi, \quad (9)$$

where  $\Xi(\mathbf{r}, t) = \exp(-i\mathbf{V}\Delta t)\Psi(\mathbf{r}, t_0)$ . The previous equation is thus equivalent to the separation of variables method such that  $x$ ,  $y$ , and  $z$  become independent and allows a natural separation in matrix form.

We approximate the exponential function to first order obtaining the following equation

$$\prod_{\eta=x,y,z} \left(1 - \frac{i\Delta t}{4} \frac{\partial^2}{\partial \eta^2}\right) \Psi = \prod_{\eta=x,y,z} \left(1 + \frac{i\Delta t}{4} \frac{\partial^2}{\partial \eta^2}\right) \Xi, \quad (10)$$

In Eq. (10), we discretize the wave function  $\Psi$  as  $\Psi(\mathbf{r}, t) \rightarrow \Psi(x_i, y_j, z_k; t^n) \rightarrow \Psi_{i,j,k}^n$  and the second derivatives of each axis onto a three dimensional Cartesian numerical grid, where the points of the grid  $\eta$  are discretized to  $\eta_k$  with  $k = 0, \dots, N$  and  $\eta = x, y, z$ . We consider Dirichlet boundary conditions, that is  $\Psi(\mathbf{r} \rightarrow \infty) = 0$ , at the boundary of the numerical grid and by arranging in matrix form, we rewrite the time-dependent Schrödinger equation as a linear algebra problem

$$\mathbf{A}_x^+ \mathbf{A}_y^+ \mathbf{A}_z^+ \Psi^{n+1} = \mathbf{A}_x^- \mathbf{A}_y^- \mathbf{A}_z^- \Xi^n \quad (11)$$

where the matrices  $A_\eta^\pm$  are given by

$$\begin{pmatrix} 1 \pm 2\nu_\eta & \mp\nu_\eta & 0 & \dots & 0 \\ \mp\nu_\eta & 1 \pm 2\nu_\eta & \mp\nu_\eta & \dots & 0 \\ 0 & \ddots & \ddots & \ddots & 0 \\ \vdots & \ddots & \ddots & \ddots & \vdots \\ 0 & \dots & \mp\nu_\eta & 1 \pm 2\nu_\eta & \mp\nu_\eta \\ 0 & \dots & 0 & \mp\nu_\eta & 1 \pm 2\nu_\eta \end{pmatrix}, \quad (12)$$

where  $\nu_\eta = i\Delta t/(4\Delta\eta^2)$ . We require that  $|\nu_\eta| < 1$  for the stability of the numerical method. At the end of the dynamics of the collision, we obtain the total evolved wave function.

### 2.3. Numerical implementation and initial conditions

We consider  $R(0) = (b, 0, z_0)$  as the point where the incident bare ion projectile starts its straight-line trajectory. We propagate the ion on the  $z$  axis, and we consider the impact parameter range as  $b \in [0.2, 10]$  and we increase it in steps of  $\Delta b = 0.2$ . Initially, the atomic hydrogen target is in the ground state and it is placed at the origin of the Cartesian numerical grid. The position of the incident bare ion projectile starts at a distance such that the electric field strength of the laser pulse is negligible. We have chosen  $\mathcal{E}(t)$  to be 1% of the value at the peak of the pulse, i.e.,  $\mathcal{E}(t_{\min})/\mathcal{E}_0 = 0.01$ , such that we reduce Stark effects when we do the projections at the final time of the collision. So, for the symmetric collisions system we consider  $\tau = 1$  fs (24.835 a.u.) obtaining  $t_{\min} = 53.3$  a.u. and since the  $H^+$  ion is placed at  $z_0 = -v_p t_{\min}$  a.u. from the target hydrogen atom, the distance where the  $H^+$  ion starts the collision is  $z_0 = -34$  a.u. for 10 keV/amu ( $v_p = 0.6328$  a.u.) impact energy collision. These assumptions fixed the size of the numerical grid as  $[-10, 20]_x \times [-15, 15]_y \times [-45, 45]_z$ . For the asymmetric system we consider  $\tau = 2$  fs (49.67 a.u.) and we get that  $t_{\min} = 106.59$  a.u. and the distance  $z_0 = -68.0$  a.u. at 10 keV/amu impact energy collision is where the  $He^{2+}$  ion starts the straight-line trajectory, so the size of the numerical grid becomes  $[-10, 20]_x \times [-15, 15]_y \times [-75, 75]_z$  for this case. Also, we use a spacing of  $\Delta\eta = 0.2$  with  $\eta = x, y, z$  and  $\Delta t = 0.06$  in both numerical grids. The initial ground state wave-function of the hydrogen atom is obtained by relaxation of the TDSE by means of imaginary time technique. We obtain the  $1s$  state in the Cartesian numerical grid with a total energy  $E(1s) = -0.4980$  a.u. for both numerical grids. The laser pulse parameters that we consider are the following: the wavelength is  $\lambda = 800$  nm ( $\omega = 0.0569$ ) because this value is suggested as a common value in an ultra-fast and intense lasers [8]. The RCLP,  $\phi$ , in the laser pulse, is an important parameter during the collision processes [6, 9], so, we consider the effect of the RCLP on the charge transfer process starting with  $\phi = 0$ , then, we increase the phase in quarters of  $\pi$  up to the value  $\phi = 2\pi$ . We report our numerical results in the Sec. 3 by performing an average on the RCLP.

For the stationary states, we use a numerical grid  $[0, 100]$  and a spacing of  $\Delta r = 0.05$ . to obtain a good description of the wave function cusp and eigen-energies.

### 2.4. State selective charge transfer cross-section

Once the solution for the  $n = 2$  for the hydrogen atom and  $n = 2, 3$  for the  $He^+$  ion are obtained, we calculate the state selective charge transfer probabilities by projecting the final wave function as follows

$$P_{n,l}(E, b) = \sum_{m=-l}^l \left| \int_V D_{n,l}(r) Y_{l,m}^* \Psi(x, y, z; t_f) dV \right|^2. \quad (13)$$

Here  $r = \sqrt{x^2 + y^2 + z^2}$  and we use a linear interpolation to match the numerical data of the radial wave functions associated to the stationary states of the hydrogen atom or  $He^+$  ion

**Table 1.** Energy eigenvalues (in eV) and expectation value  $\langle r \rangle$  (in a.u.) for hydrogen atom and  $\text{He}^+$  ion as obtained with our numerical method for  $n = 2$ , and 3. The results are compared to the exact analytic result  $\langle r \rangle^* = [3n^2 - l(l + 1)]/2Z$  and  $-13.606Z^2/n^2$  for a hydrogen atom.

Hydrogen atom					$\text{He}^+$ ion			
State	$\langle r \rangle$	$\langle r \rangle^*$	$E_{nl}$	$E_{\text{exact}}$	$\langle r \rangle$	$\langle r \rangle^*$	$E_{nl}$	$E_{\text{exact}}$
2s	6.000	6.0	-3.400	-3.402	3.000	3.00	-13.604	-13.606
2p	4.999	5.0	-3.400	-3.402	2.499	2.50	-13.606	-13.606
3s	13.500	13.5	-1.511	-1.512	6.751	6.75	-6.047	-6.047
3p	12.499	12.5	-1.511	-1.512	6.248	6.25	-6.047	-6.047
3d	10.499	10.5	-1.511	-1.512	5.249	5.25	-6.046	-6.047

with the total wave function  $\Psi$  at the final time of the dynamics in Cartesian coordinates. We calculate the state selective charge transfer cross-section as

$$\sigma_{nl}(E) = 2\pi \int_0^\infty P_{n,l}(E, b) b db, \quad (14)$$

where the upper limit is replaced by a cut-off value determined by the size of the numerical grid.

### 3. Results

#### 3.1. Stationary states of the hydrogen atom and $\text{He}^+$ ion

To assess the validity of our numerical approach, the electron position expectation value  $\langle r \rangle$  and eigen-energies of the stationary states of the neutral hydrogen atom and  $\text{He}^+$  are obtained by solving numerically the TISE. In table 1, we show our numerical results for the expectation value  $\langle r \rangle$  and compare with the analytic result  $\langle r \rangle = [3n^2 - l(l + 1)]/2Z$  a.u. for the  $n = 2$  and 3 states of atomic hydrogen. Also, the eigen-energy values are compared to the analytical value of  $-13.606Z^2/n^2$  eV. We have a good agreement with all analytic quantities. Thus, within our numerical grid, we are confident that we have a proper wave function description of the hydrogen atom and  $\text{He}^+$  ion states to calculate the projections to obtain the charge transfer probabilities.

#### 3.2. Charge transfer cross-section into the $n = 2$ states of $\text{H}^+ + \text{H}$

The  $\text{H}^+ + \text{H}$  collision system is a symmetric system, the target and the projectile have the same energy levels. In Fig. 1, we show the electron transfer cross section results for the  $n = 2$  shell. We observe in the Fig. 1(a) that our 2s state laser-free results (solid line) have a good agreement with the theoretical results reported by Winter [10], Lüdde et al. [11], Cheshire et al. [12] and Fritsch et al. [13] in the high energy region for up to 3 keV/amu. For energies lower than 3 keV/amu we have a discrepancy when comparing to the experimental data that we attribute to the straight-line trajectory approximation. For the 2p state we show, in Fig. 1(b), the good agreement between our laser-free numerical results to those reported by the theoretical methods of Winter [10], Lüdde et al. [11], Cheshire et al. [12] and Fritsch et al. [13], and with experimental data by Barnett et al. [16] and Morgan et al. [14]. Also, in the same figures, we compare our numerical results for the 2s and 2p states for the laser case for a 1 fs laser pulse width. We notice a minimal effect for all the collision energies on the charge transfer process in agreement to Ferrante et al. [7] within the error bars of the experiment. As from the results reported in figure 1, we observe that the laser pulse affects the  $2p_{\pm 1}$  states of the projectile, and the laser pulse increases the probability of charge transfer, but for the 2s state the effect is negligible.

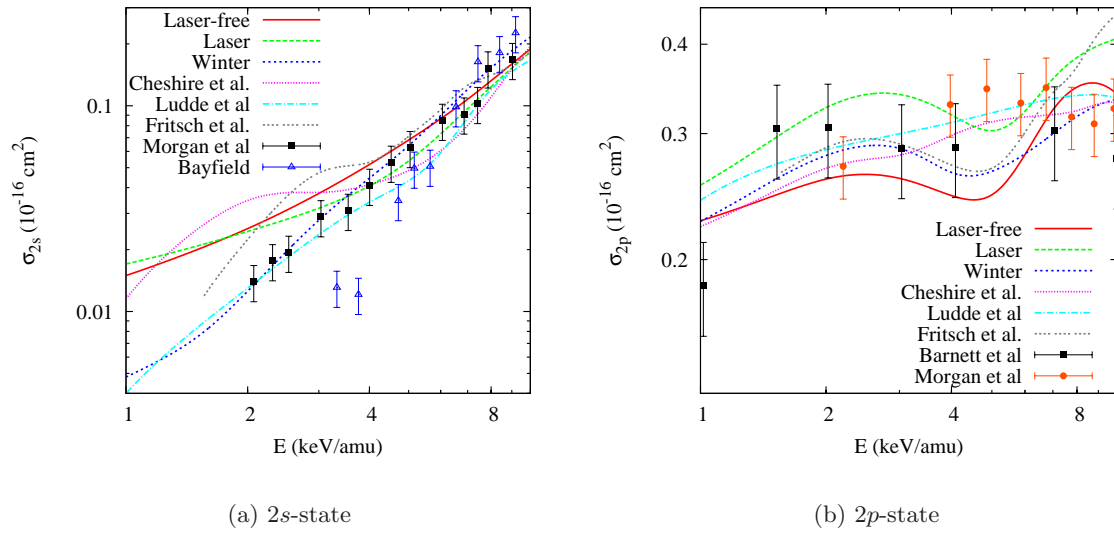


**Figure 1.** We show the effect of the laser pulse on the 2s (Fig. 1(a)) and 2p (Fig. 1(b)) state charge transfer process of the symmetric system  $H^+ + H$  by comparing our laser-free and laser cross-section. We compare with the laser-free theoretical methods by Winter [10], Lüdde et al. [11], Cheshire et al. [12] and Fritsch et al. [13]. Also, we compare with laser-free experimental data by Morgan et al. [14], Bayfield [15] and Barnett et al. [16].

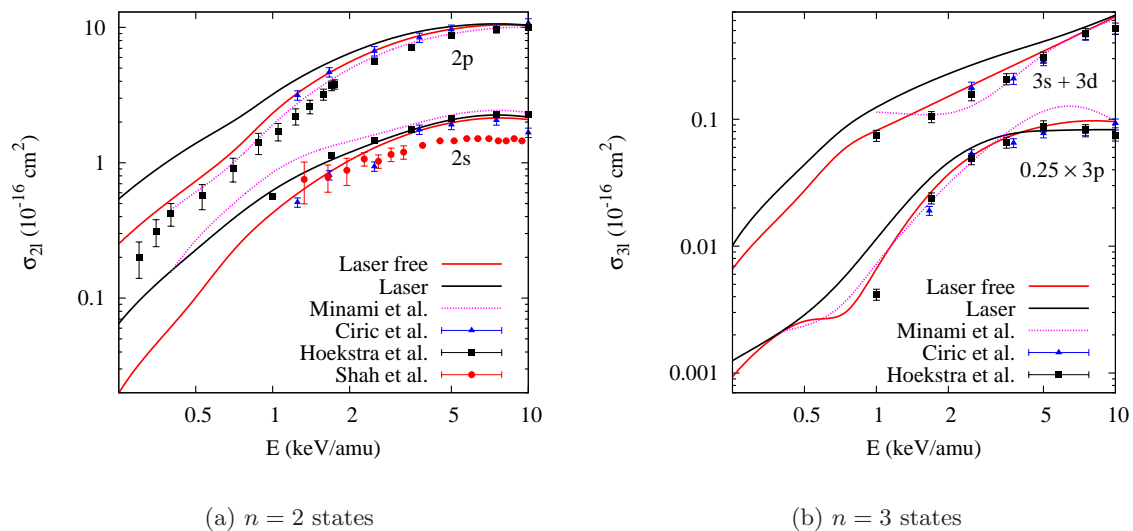


**Figure 2.** In Fig. 2(a) and Fig. 2(b) we report the  $n = 2$  and  $n = 3$  charge transfer cross section, respectively, for the  $He^{2+} + H$  collision system as a function of the projectile kinetic energy for the laser and laser-free cases. We compare our laser-free results with the theoretical results by Minami et al. [17] and the experimental measurements for laser free collisions by Ćirić et al. [18] and Hoekstra et al. [19].



### 3.3. $n = 2$ and 3 states charge transfer cross-section of $\text{He}^{2+} + \text{H}$ system

Finally, we obtain the probability for  $n = 2, 3$  charge transfer of the asymmetric system  $\text{He}^{2+} + \text{H}$  using Eq. (14), for the laser-free and for the laser assisted collision. In Fig. 2(a) we report our numerical results for the  $n = 2, 3$  charge transfer cross-section for both cases. For the laser-free case, we compare our numerical results with the theoretical results by Minami et al. [17] and experimental measurements by Ćirić et al. [18] and Hoekstra et al. [19]. We notice a good agreement between our numerical results and those reported in the literature. In Fig. 2(b), we notice an increase of the  $n = 3$  charge transfer cross-section in the range 0.25-1 keV. In particular, the value of the  $3s + 3d$  state charge transfer cross-section is increased by a factor of two in the range 0.25-3 keV. The laser pulse has a greater effect on this system because the coupling of the projectile and the target are different and the Stark effect in the collisions is not the same for both particles as in the symmetrical collision system case.

## 4. Summary

In this paper we have presented our first results of the study of laser-assisted collision of asymmetric and symmetric collision systems. We used the finite-differences method to solve the TISE finding a good agreement between our numerical results for the energy eigenvalues of the Hydrogen atom and  $\text{He}^+$  ion with the hydrogen analytical values. We have analyzed the effect of an ultra-fast, short and intense laser pulse on the state-selective charge transfer process of the both collisions systems finding a minimal effect on the symmetrical system and a larger effect on the asymmetrical system. We have showed that our numerical results for the  $n = 2$  charge transfer cross-section of the  $\text{H}^+ + \text{H}$  for the laser-free case and for the laser assistance, finding a good agreement with the laser-free experimental data. We have found an appreciable effect of the laser assisted charge transfer process of the asymmetric system  $\text{He}^{2+} + \text{H}$  for low impact energy collisions.

In conclusion, for the symmetric collision systems the laser effect is minimal on the total and  $n = 2$  charge transfer process, but for the  $\text{He}^{2+} + \text{H}$  collision systems the laser enhances the total [6, 9] and  $n = 2$  charge transfer process in the low impact energy collision range. Further work is in progress to find the effect of the laser wave-length and intensity, as well as the polarization to characterize in full the effect of laser assisted collision in the symmetry of the laser-assisted ion-atom collision.

We acknowledge support from grant PAPIIT IN 101-611 and CONACyT (Ph.D. scholarship). We thank the ICF-UNAM computer center for assistance.

## References

- [1] Isler R C and Crume E C 1978 *Phys. Rev. Lett.* **41**(19) 1296–1300
- [2] Hsu Y P, Kimura M and Olson R E 1985 *Phys. Rev. A* **31** 576
- [3] Madsen L B, Hansen J P and Kocbach L 2002 *Phys. Rev. Lett.* **89** 093202
- [4] Kirchner T 2004 *Phys. Rev. A* **69** 063412
- [5] Niederhausen T and Thumm U 2006 *Phys. Rev. A* **73**(4) 041404
- [6] Anis F, Roudnev V, Cabrera-Trujillo R and Esry B D 2006 *Phys. Rev. A* **73** 043414
- [7] Ferrante G, Casico L L and Spagnolo B 1981 *Journal of Physics B: Atomic and Molecular Physics* **14** 3961
- [8] Wall K A and Sanchez A 1990 *The Lincoln laboratory journal* **3**
- [9] Kirchner T 2002 *Phys. Rev. Lett.* **89** 093203
- [10] Winter T G 2009 *Phys. Rev. A* **80** 032701
- [11] Ludde H J and Dreizler R M 1982 *Journal of Physics B: Atomic and Molecular Physics* **15** 2703

- [12] Cheshire I M, Gallaher D F and Taylor A J 1970 *Journal of Physics B: Atomic and Molecular Physics* **3** 813
- [13] Fritsch W and Lin C D 1982 *Phys. Rev. A* **26** 762–769
- [14] Morgan T J, Geddes J and Gilbody H B 1973 *Journal of Physics B: Atomic and Molecular Physics* **6** 2118
- [15] Bayfield J E 1969 *Phys. Rev.* **185** 105–112
- [16] Barnett C F 1990 *Oak Ridge National Laboratory Report* **6068**
- [17] Minami T, Lee T G, Pindzola M S and Schultz D R 2008 *Journal of Physics B: Atomic, Molecular and Optical Physics* **41** 135201
- [18] Ćirić D, Dijkkamp D, Vlieg E and de Heer F J 1985 *Journal of Physics B: Atomic and Molecular Physics* **18** 4745
- [19] Hoekstra R, de Heer F J and Morgenstern R 1991 *Journal of Physics B: Atomic, Molecular and Optical Physics* **24** 4025